REVISTA DE LA UNIÓN MATEMÁTICA ARGENTINA
Published online: October 8, 2025
https://doi.org/10.33044/revuma.4665

A HIGH-ACCURACY COMPACT FINITE DIFFERENCE SCHEME FOR TIME-FRACTIONAL DIFFUSION EQUATIONS

XINDONG ZHANG, HANXIAO WANG, ZIYANG LUO, AND LEILEI WEI

Abstract. We propose a compact finite difference (CFD) scheme for the solution of time-fractional diffusion equations (TFDE) with the Caputo–Fabrizio derivative. The Caputo–Fabrizio derivative is discussed in the time direction and is discretized by a special discrete scheme. The compact difference operator is introduced in the space direction. We prove the unconditional stability and convergence of the proposed scheme. We show that the convergence order is $O(\tau^3 + h^4)$, where τ and h are the temporal stepsize and spatial stepsize, respectively. Our main purpose is to show that the Caputo–Fabrizio derivative without singular term can improve the accuracy of the discrete scheme. Numerical examples demonstrate the efficiency of the proposed method, and the numerical results agree well with the theoretical predictions.

1. Introduction

In recent decades, fractional calculus has become more widely used in different engineering fields [7, 25, 4, 18], and the study of related fractional differential equations (FDEs) has become a focus of many scholars. There are various forms of fractional derivative; commonly used ones include Caputo, Riemann–Liouville (R-L) and Grünwald–Letnikov (G-L). For more details refer to [17, 20, 26, 11, 30, 23, 28]. It is known that analytical solutions for fractional differential equations are difficult to obtain; however, many scholars still seek such solutions [33, 19, 24]. Compared with analytical methods, numerical methods are more important in practical applications, and results for fractional differential equations obtained numerically can be found in [41, 38, 14, 9].

The diffusion equation is a partial differential equation used to describe changes in the density of matter in diffusion phenomena. It is also commonly used to model similar processes, such as the spread of alleles in population genetics. If we replace

2020 *Mathematics Subject Classification.* Primary 65N06; Secondary 65N12.

Key words and phrases. time-fractional diffusion equation, Caputo–Fabrizio derivative, compact finite difference, stability, error estimate.

This work was supported by Guizhou University of Finance and Economics Innovation Exploration and Academic Emerging Project (No. 2024XSXMB13) and the Natural Science Foundation of Xinjiang Uygur Autonomous Region (No. 2022D01E13).

the integer-order derivative in the time direction with a fractional derivative of order α ($0 < \alpha < 1$), then a diffusion equation with a time-fractional derivative can be obtained that can more accurately describe some anomalous diffusion phenomena. TFDEs are derived by considering continuous-time random-walk problems, which are in general non-Markovian processes. The physical interpretation of the fractional derivative is that it represents a degree of memory in the diffusing material [16, 27]. There are many results on the numerical solutions of TFDEs. For example, in [15], Gorenflo et al. considered the numerical solution of TFDEs in fractional Sobolev spaces. The authors of [29] introduced some initial-boundary-value problems for TFDEs in open bounded one-dimensional domains. The authors of [39] proposed a new compact alternating direction implicit method for solving two-dimensional time-fractional diffusion equation with the Caputo–Fabrizio (C-F) derivative.

The C-F derivative was first presented by Caputo and Fabrizio [6]. This operator is important and interesting for describing the behavior of some complex physical materials. Another interesting aspect for the C-F derivative is that it can provide new perspectives for some areas of mechanical phenomena. This derivative is a promising differentiation operator and it has been widely applied to several models arising in many fields, such as biology, physics, control systems, materials science, fluid dynamics, and real-world problems [3, 5]. Up to now, there are many results about C-F derivative. In [2], a new discretization of the Caputo–Fabrizio derivative was discussed. The authors of [12] introduced a numerical method for TFDEs based on the C-F operator, in which a finite difference method and a spectral method were used. For the latest results about the C-F derivative, one can refer to [21, 32, 31, 35, 1, 36, 10], among others.

The CFD operator has good applications for solving FDEs. It has been studied and applied by many scholars. In [8], the CFD method was used to obtain a fully discrete implicit scheme for the fractional diffusion equation. In [42], the compact difference scheme for distributed-order time-fractional diffusion-wave equation on bounded domains was considered by Ye et al. The authors of [34] presented a class of new compact difference schemes, which were used for solving the fourth-order time-fractional sub-diffusion equation. In [40], Wang and Vong studied CFD schemes for two types of fractional partial differential equations. In [13], a high-order accurate scheme by using compact difference operator was proposed for time-fractional advection-diffusion equations. Among the numerous numerical methods for solving FDEs, CFD proves to be an effective method for constructing high-order schemes.

Therefore, in this paper, we want to construct high-order numerical schemes for solving TFDEs by CFD. The TFDE is as follows:

$$\begin{cases} {}_0^{\mathrm{CF}}D_t^{\alpha} u(x,t) = a\dfrac{\partial^2 u}{\partial x^2} + f(x,t), & (x,t) \in (0,L)\times(0,T), \\ u(x,t)|_{t=0} = \varphi(x), & x \in \Omega = [0,L], \\ u(0,t) = u(L,t) = 0, & t \in [0,T], \end{cases} \tag{1.1}$$

where $a > 0$ represents the diffusion coefficient, L is the length of the space, and T is the termination time. $f(x,t)$ and $\varphi(x)$ are all given and sufficiently smooth functions. We use ${}_0^{\mathrm{CF}}D_t^\alpha$ to denote the C-F derivative [6], which is defined by

$${}_0^{\mathrm{CF}}D_t^\alpha u(t) = \frac{1}{1-\alpha}\int_0^t u'(s)e^{-\frac{\alpha}{1-\alpha}(t-s)}\,\mathrm{d}s = \frac{1}{1-\alpha}\int_0^t u'(s)e^{-\varrho(t-s)}\,\mathrm{d}s,$$

where $\varrho = \frac{\alpha}{1-\alpha}$ and $0 < \alpha < 1$.

The rest of the paper is organized as follows. In Section 2, some notations will be given and a discrete scheme will be proposed for the diffusion equation (1.1). The stability and error estimation of the proposed discrete scheme will be discussed in Section 3. In Section 4, in order to confirm the efficiency and usefulness of the proposed discrete scheme, some numerical experiments will be considered. Finally, some conclusions will be given in Section 5.

2. Construction of the numerical scheme for TFDE

In the present section, the construction of a discrete scheme for (1.1) will be considered. For the development of our discrete scheme, we provide some notations that will be used in this section and others. For given positive integers M and N, let $x_j = jh$, $j = 0, 1, \ldots, M$, where $h = L/M$ is the space stepsize, and let $t_n = n\tau$, $n = 0, 1, \ldots, N$, where $\tau = T/N$ is the time stepsize. We use $[N]$ to denote the set $\{1, 2, \ldots, N\}$. We define $u_j^n = u(x_j, t_n)$ and $f_j^n = f(x_j, t_n)$. We denote by $V_h = \{V \mid V = (V_0, V_1, \ldots, V_M),\ V_0 = V_M = 0\}$ the grid function space. For any functions $V, W \in V_h$, let

$$\delta_x V_{j-\frac{1}{2}} = \frac{V_j - V_{j-1}}{h}, \quad \delta_x V_{j+\frac{1}{2}} = \frac{V_{j+1} - V_j}{h},$$
$$\delta_x^2 V_j = \frac{\delta_x V_{j+\frac{1}{2}} - \delta_x V_{j-\frac{1}{2}}}{h} = \frac{V_{j+1} - 2V_j + V_{j-1}}{h^2}.$$

Define the inner products and Sobolev norms (or seminorms)

$$(V, W) = h\sum_{j=1}^{M-1} V_j\overline{W_j}, \quad \|V\| = \sqrt{(V,V)},$$

$$\langle \delta_x V_j, \delta_x W_j\rangle = h\sum_{j=1}^{M} \delta_x V_{j-\frac{1}{2}}\overline{\delta_x W_{j-\frac{1}{2}}}, \quad (\delta_x^2 V_j, \delta_x^2 W_j) = h\sum_{j=1}^{M-1}\delta_x^2 V_j\overline{\delta_x^2 W_j},$$

$$(V, W)_A = \langle \delta_x V_j, \delta_x W_j\rangle - \frac{h^2}{12}(\delta_x^2 V_j, \delta_x^2 W_j), \quad \|V\|_A = \sqrt{(V,V)_A}.$$

We use $\mathcal{H}$ to represent a compact operator, which has the following form:

$$\mathcal{H}u_j^n = \begin{cases} \frac{1}{12}u_{j-1}^n + \frac{10}{12}u_j^n + \frac{1}{12}u_{j+1}^n = \left(1 + \frac{h^2}{12}\delta_x^2\right)u_j^n, & j \in [M-1], \\ u_j^n, & j = 0 \text{ or } M. \end{cases} \tag{2.1}$$

For convenience, we allow C to represent different values at different positions. Next, we introduce some lemmas that are helpful for understanding the construction of our discrete scheme.

Lemma 2.1 ([13])**.** *Let $\mathcal{H}$ be the compact operator defined in* (2.1)*. Suppose $u(x) \in C^6(\Omega)$, then one has*

$$\mathcal{H}u_{xx}(x_j, t_n) = \delta_x^2 u_j^n + O(h^4),$$

where h is the space stepsize and $j \in [M]$.

Lemma 2.2 ([37])**.** *Let $\varrho = \frac{\alpha}{1-\alpha}$ with $0 < \alpha < 1$. Let $u(t)$ be a sufficiently smooth function for $t > 0$. Then*

$$ {}_0^{\mathrm{CF}}D_t^\alpha u^n = \lambda \sum_{k=1}^{n} e^{-\varrho(n-k)\tau}(u^k - u^{k-1}) + \beta \sum_{k=2}^{n} e^{-\varrho(n-k)\tau}(u^k - 2u^{k-1} + u^{k-2}) + O(\tau^3),$$

where $\lambda = \frac{1-e^{-\varrho\tau}}{\alpha\tau}$ and $\beta = \frac{2(\alpha-1)(1-e^{-\varrho\tau}) + \alpha\tau(1+e^{-\varrho\tau})}{2\alpha^2\tau^2}$.

By Lemma 2.2, we have

$$\begin{aligned} {}_0^{\mathrm{CF}}D_t^\alpha u^n =& -(\lambda e^{-\varrho\tau} - \beta)e^{-\varrho(n-2)\tau}u^0 + \big(\lambda e^{-2\varrho\tau} - ((\lambda + 2\beta)e^{-\varrho\tau} - \beta)\big)e^{-\varrho(n-3)\tau}u^1 \\ & - \sum_{k=2}^{n-2}(1 - e^{-\varrho\tau})((\lambda+\beta)e^{-\varrho\tau} - \beta)e^{-\varrho(n-k-2)\tau}u^k \\ & - ((\lambda+\beta)(1 - e^{-\varrho\tau}) + \beta)u^{n-1} + (\lambda+\beta)u^n + O(\tau^3). \end{aligned}$$

Let $A_1 = (\lambda + 2\beta)e^{-\varrho\tau} - \beta$, $A_2 = (1 - e^{-\varrho\tau})((\lambda+\beta)e^{-\varrho\tau} - \beta)$, and $A_3 = (\lambda + \beta)(1 - e^{-\varrho\tau}) + \beta$. By the definition of the compact operator $\mathcal{H}$ and Lemmas 2.1 and 2.2, one has

$$\begin{cases} (\lambda+\beta)\mathcal{H}u_j^n - a\delta_x^2 u_j^n = (\lambda e^{-\varrho\tau} - \beta)e^{-\varrho(n-2)\tau}\mathcal{H}u_j^0 - (\lambda e^{-2\varrho\tau} - A_1)e^{-\varrho(n-3)\tau}\mathcal{H}u_j^1 \\ \qquad + A_2 \sum_{k=2}^{n-2} e^{-\varrho(n-k-2)\tau}\mathcal{H}u_j^k + A_3\mathcal{H}u_j^{n-1} + \mathcal{H}f_j^n + R_j^n, \\ \qquad\qquad j \in [M-1],\ n \in [N-1], \\ u_j^0 = \varphi(x_j), \qquad 0 \le j \le M, \\ u_0^n = u_M^n = 0, \qquad n \in [N], \end{cases} \tag{2.2}$$

where $\|R_j^n\| \le C(\tau^3 + h^4)$.

We use U_j^n to represent the numerical approximation of $u(x,t)$ at the mesh point (x_j, t_n). If we ignore the truncation error term R_j^n in (2.2), then we get the CFD scheme for (1.1) as follows:

$$\begin{cases} (\lambda+\beta)\mathcal{H}U_j^n - a\delta_x^2 U_j^n = (\lambda e^{-\varrho\tau} - \beta)e^{-\varrho(n-2)\tau}\mathcal{H}U_j^0 \\ \qquad - (\lambda e^{-2\varrho\tau} - A_1)e^{-\varrho(n-3)\tau}\mathcal{H}U_j^1 \\ \qquad + A_2 \sum_{k=2}^{n-2} e^{-\varrho(n-k-2)\tau}\mathcal{H}U_j^k + A_3\mathcal{H}U_j^{n-1} + \mathcal{H}f_j^n, \\ \qquad\qquad j \in [M-1],\ n \in [N-1], \\ U_j^0 = \varphi(x_j), \qquad 0 \le j \le M, \\ U_0^n = U_M^n = 0, \qquad n \in [N]. \end{cases} \tag{2.3}$$

3. Stability analysis and error estimates

The main purpose of this section is to provide and prove the stability and error estimation for the discrete scheme (2.3). Next, we introduce some lemmas that are helpful for understanding the proof of our main results. We will ignore the subscript j in the following discussion.

Lemma 3.1 ([44, 22]). *If $V, W \in V_h$, then $(\delta_x^2 V, W) = -\langle \delta_x V, \delta_x W\rangle$.*

Lemma 3.2. *For any grid function $V, W \in V_h$,*

$$-(\delta_x^2 V, \mathcal{H}W) = (V, W)_A.$$

Proof. Applying the definition of the operator $\mathcal{H}$, we get

$$-(\delta_x^2 V, \mathcal{H}W) = -(\delta_x^2 V, (1 + \frac{h^2}{12}\delta_x^2)W) = -(\delta_x^2 V, W) - \frac{h^2}{12}(\delta_x^2 V, \delta_x^2 W).$$

By Lemma 3.1, $(\delta_x^2 V, W) = -\langle \delta_x V, \delta_x W\rangle$. It follows that

$$-(\delta_x^2 V, \mathcal{H}W) = \langle \delta_x V, \delta_x W\rangle - \frac{h^2}{12}(\delta_x^2 V, \delta_x^2 W) = (V, W)_A.$$

Then the proof is complete. □

Lemma 3.3 ([43]). *For any grid function $U \in V_h$, $\frac{1}{3}\|U\|^2 \le \|\mathcal{H}U\|^2 \le \|U\|^2$.*

The proof of the following lemma is simple, and we will omit its process here.

Lemma 3.4. *Let $\varrho = \frac{\alpha}{1-\alpha}$ with $0 < \alpha < 1$. Then*

$$\sum_{k=1}^{n-1} e^{-\varrho(n-1-k)\tau}(1 - e^{-\varrho\tau}) < 1.$$

Lemma 3.5 ([37]). *Let $\varrho = \frac{\alpha}{1-\alpha}$ with $0 < \alpha < 1$, and let*

$$T_k^n = \big(2(\alpha-1)(1 - e^{-\varrho\tau}) + \alpha\tau(1 + e^{-\varrho\tau})\big)e^{-\varrho(n-k)\tau}, \quad 2 \le k \le n.$$

Then

$$T_n^n > T_{n-1}^n > \cdots > T_k^n > T_{k-1}^n > \cdots > T_2^n > 0.$$

Lemma 3.6. *Let $0 < \alpha < 1$ with $\varrho = \frac{\alpha}{1-\alpha}$. Then*

$$0 < \frac{A_2}{\lambda + \beta}\sum_{k=2}^{n-2} e^{-\varrho(n-k-2)\tau} < 1,$$

where

$$\lambda = \frac{1 - e^{-\varrho\tau}}{\alpha\tau}, \quad \beta = \frac{2(\alpha-1)(1 - e^{-\varrho\tau}) + \alpha\tau(1 + e^{-\varrho\tau})}{2\alpha^2\tau^2},$$
$$A_2 = (1 - e^{-\varrho\tau})((\lambda + \beta)e^{-\varrho\tau} - \beta).$$

Proof. Since $A_2 = (1 - e^{-\varrho\tau})((\lambda+\beta)e^{-\varrho\tau} - \beta)$, we get

$$\frac{A_2}{\lambda+\beta}\sum_{k=2}^{n-2} e^{-\varrho(n-k-2)\tau} = \frac{(\lambda+\beta)e^{-\varrho\tau}-\beta}{\lambda+\beta}\sum_{k=2}^{n-2}(1-e^{-\varrho\tau})e^{-\varrho(n-k-2)\tau}.$$

Firstly, we will show that $0 < \frac{(\lambda+\beta)e^{-\varrho\tau}-\beta}{\lambda+\beta} < 1$. For this purpose, we consider $(\lambda+\beta)e^{-\varrho\tau} - \beta$ to be expanded into the following form:

$$\begin{aligned}
&(\lambda+\beta)e^{-\varrho\tau} - \beta \\
&\quad= \lambda e^{-\varrho\tau} + \beta(e^{-\varrho\tau} - 1) \\
&\quad= \frac{e^{-\varrho\tau} - e^{-2\varrho\tau}}{\alpha\tau} + \frac{(2\alpha-2)(2e^{-\varrho\tau} - e^{-2\varrho\tau} - 1) + \alpha\tau(e^{-2\varrho\tau} - 1)}{2\alpha^2\tau^2} \\
&\quad= \frac{(2-2\alpha-\alpha\tau)(e^{-2\varrho\tau} - 2e^{-\varrho\tau} + 1)}{2\alpha^2\tau^2}.
\end{aligned}$$

For $0 < \alpha < 1$, we know that $\lim_{\tau\to 0}(2-2\alpha-\alpha\tau) > 0$ and $\lim_{\tau\to 0}(e^{-2\varrho\tau} - 2e^{-\varrho\tau} + 1) > 0$; then we obtain $(\lambda+\beta)e^{-\varrho\tau} - \beta > 0$. By Lemma 3.5, we know that $\beta > 0$. If $\tau \to 0$, we get

$$\lambda + \beta - ((\lambda+\beta)e^{-\varrho\tau} - \beta) = \lambda(1 - e^{-\varrho\tau}) + \beta(2 - e^{-\varrho\tau}) > 0.$$

This means that $\lambda + \beta > 0$, and we get $0 < \frac{(\lambda+\beta)e^{-\varrho\tau}-\beta}{\lambda+\beta} < 1$.

By Lemma 3.4, we know that $0 < \sum_{k=2}^{n-2}(1-e^{-\varrho\tau})e^{-\varrho(n-k-2)\tau} < 1$. Thus,

$$0 < \frac{A_2}{\lambda+\beta}\sum_{k=2}^{n-2} e^{-\varrho(n-k-2)\tau} < 1.$$

This completes the proof. □

By the proof of Lemma 3.6, we have $(\lambda+\beta)e^{-\varrho\tau} - \beta > 0$. Hence, the following remark is straightforward.

Remark 3.7. Let $A_1 = (\lambda+2\beta)e^{-\varrho\tau} - \beta$, $A_2 = (1-e^{-\varrho\tau})((\lambda+\beta)e^{-\varrho\tau} - \beta)$ and $A_3 = (\lambda+\beta)(1-e^{-\varrho\tau}) + \beta$. Then:

(i) $A_1 > 0$, $A_2 > 0$ and $A_3 > 0$.
(ii) $\lambda e^{-2\varrho\tau} - A_1 < 0$.

First we will give the proof of stability for the discrete scheme (2.3).

Theorem 3.8. *Let U^n be the solution of* (2.3) *with respect to the initial and boundary conditions. Then*

$$\|U^n\| \le C\Big(\|U^0\| + \max_{1\le s\le n}\|f^s\|\Big),$$

where C is a positive constant and $n \in [N]$.

Proof. By (2.3), we get

$$(\lambda+\beta)\mathcal{H}U^n - a\delta_x^2 U^n = (\lambda e^{-\varrho\tau}-\beta)e^{-\varrho(n-2)\tau}\mathcal{H}U^0 - (\lambda e^{-2\varrho\tau}-A_1)e^{-\varrho(n-3)\tau}\mathcal{H}U^1 + A_2\sum_{k=2}^{n-2} e^{-\varrho(n-k-2)\tau}\mathcal{H}U^k + A_3\mathcal{H}U^{n-1} + \mathcal{H}f^n. \tag{3.1}$$

Multiplying both sides of (3.1) by $\mathcal{H}U^n$ and integrating on Ω, we obtain

$$\begin{aligned}(\lambda+\beta)&(\mathcal{H}U^n,\mathcal{H}U^n) - a(\delta_x^2 U^n,\mathcal{H}U^n)\\ &= (\lambda e^{-\varrho\tau}-\beta)e^{-\varrho(n-2)\tau}(\mathcal{H}U^0,\mathcal{H}U^n) - (\lambda e^{-2\varrho\tau}-A_1)e^{-\varrho(n-3)\tau}(\mathcal{H}U^1,\mathcal{H}U^n)\\ &\quad + A_2\Big(\sum_{k=2}^{n-2} e^{-\varrho(n-k-2)\tau}\mathcal{H}U^k,\mathcal{H}U^n\Big) + A_3(\mathcal{H}U^{n-1},\mathcal{H}U^n) + (\mathcal{H}f^n,\mathcal{H}U^n).\end{aligned}$$

By Lemma 3.2, $-a(\delta_x^2 U^n,\mathcal{H}U^n) = a(U^n,U^n)_A \geq 0$. Then, we have

$$\begin{aligned}(\lambda+\beta)&(\mathcal{H}U^n,\mathcal{H}U^n)\\ &\leq (\lambda e^{-\varrho\tau}-\beta)e^{-\varrho(n-2)\tau}(\mathcal{H}U^0,\mathcal{H}U^n) - (\lambda e^{-2\varrho\tau}-A_1)e^{-\varrho(n-3)\tau}(\mathcal{H}U^1,\mathcal{H}U^n)\\ &\quad + A_2\Big(\sum_{k=2}^{n-2} e^{-\varrho(n-k-2)\tau}\mathcal{H}U^k,\mathcal{H}U^n\Big) + A_3(\mathcal{H}U^{n-1},\mathcal{H}U^n) + (\mathcal{H}f^n,\mathcal{H}U^n).\end{aligned} \tag{3.2}$$

By Remark 3.7, we have $A_2>0$, $A_3>0$ and $-(\lambda e^{-2\varrho\tau}-A_1)>0$. In (3.2), if $\lambda e^{-\varrho\tau}-\beta>0$, we get

$$(\lambda+\beta)\|\mathcal{H}U^n\| \leq (\lambda e^{-\varrho\tau}-\beta)e^{-\varrho(n-2)\tau}\|\mathcal{H}U^0\| - (\lambda e^{-2\varrho\tau}-A_1)e^{-\varrho(n-3)\tau}\|\mathcal{H}U^1\| + A_2\sum_{k=2}^{n-2} e^{-\varrho(n-k-2)\tau}\|\mathcal{H}U^k\| + A_3\|\mathcal{H}U^{n-1}\| + \|\mathcal{H}f^n\|, \tag{3.3}$$

and if $\lambda e^{-\varrho\tau}-\beta\leq 0$, we have

$$\begin{aligned}(\lambda+\beta)\|\mathcal{H}U^n\| &\leq -(\lambda e^{-2\varrho\tau}-A_1)e^{-\varrho(n-3)\tau}\|\mathcal{H}U^1\|\\ &\quad + A_2\sum_{k=2}^{n-2} e^{-\varrho(n-k-2)\tau}\|\mathcal{H}U^k\| + A_3\|\mathcal{H}U^{n-1}\| + \|\mathcal{H}f^n\|.\end{aligned} \tag{3.4}$$

Next, we want to prove by mathematical induction the inequality

$$\|\mathcal{H}U^n\| \leq C\Big(\|\mathcal{H}U^0\| + \max_{1\leq s\leq n}\|\mathcal{H}f^s\|\Big),$$

where $n\in[N]$.

From the proof of Lemma 3.6, we see that $\lambda+\beta>0$. If $n=1$ and $\lambda e^{-\varrho\tau}-\beta>0$, then by (3.3) we have

$$\begin{aligned}(\lambda+\beta)\|\mathcal{H}U^1\| &\leq (\lambda e^{-\varrho\tau}-\beta)e^{\varrho\tau}\|\mathcal{H}U^0\| - (\lambda e^{-2\varrho\tau}-A_1)e^{2\varrho\tau}\|\mathcal{H}U^1\|\\ &\quad + A_3\|\mathcal{H}U^0\| + \|\mathcal{H}f^1\|,\end{aligned}$$

i.e.,

$$(2\lambda+\beta-A_1e^{2\varrho\tau})\|\mathcal{H}U^1\| \le (\lambda-\beta e^{\varrho\tau}+A_3)\|\mathcal{H}U^0\|+\|\mathcal{H}f^1\|. \tag{3.5}$$

For the above formula, we need to verify that

$$2\lambda+\beta-A_1e^{2\varrho\tau} \ge c>0. \tag{3.6}$$

By (3.6), we get

$$2\lambda+\beta-A_1e^{2\varrho\tau}=\lambda(2-e^{\varrho\tau})+\beta(1+e^{2\varrho\tau}-2e^{\varrho\tau}).$$

From Lemma 3.5, $\beta>0$; therefore, $\beta(1+e^{2\varrho\tau}-2e^{\varrho\tau})=\beta(e^{\varrho\tau}-1)^2>0$. For the term $\lambda(2-e^{\varrho\tau})$, we get

$$\lambda(2-e^{\varrho\tau})=\frac{(1-e^{-\varrho\tau})(2-e^{\varrho\tau})}{\alpha\tau}. \tag{3.7}$$

In (3.7), as $\tau\to 0$, we get $e^{-\varrho\tau}\to 1^-$ and $e^{\varrho\tau}\to 1^+$, which means that

$$\lim_{\tau\to 0}(1-e^{-\varrho\tau})>0 \quad \text{and} \quad \lim_{\tau\to 0}(2-e^{\varrho\tau})>0,$$

i.e., $(1-e^{-\varrho\tau})(2-e^{\varrho\tau})>0$. Thus, as the parameter is given, $2\lambda+\beta-A_1e^{2\varrho\tau}\ge c>0$ holds. Combining $2\lambda+\beta-A_1e^{2\varrho\tau}\ge c>0$ and $\lambda-\beta e^{\varrho\tau}+A_3>0$, we arrive at

$$0<\frac{\lambda-\beta e^{\varrho\tau}+A_3}{2\lambda+\beta-A_1e^{2\varrho\tau}}<C.$$

In summary, (3.5) can be written as

$$\|\mathcal{H}U^1\|\le C(\|\mathcal{H}U^0\|+\|\mathcal{H}f^1\|). \tag{3.8}$$

Similarly, if $n=1$ and $\lambda e^{-\varrho\tau}-\beta\le 0$, by (3.4), we also get the same result as (3.8).

Assume that

$$\|\mathcal{H}U^k\|\le C_{k-1}\Big(\|\mathcal{H}U^0\|+\max_{1\le s\le k}\|\mathcal{H}f^s\|\Big)$$

holds as $k=2,3,\dots,n-1$, where C_{k-1} is a positive constant and independent of n. Then, for $k=n$, we want to prove the following inequality:

$$\|\mathcal{H}U^n\|\le C\Big(\|\mathcal{H}U^0\|+\max_{1\le s\le n}\|\mathcal{H}f^s\|\Big).$$

For $k=n$ and $\lambda e^{-\varrho\tau}-\beta>0$, by (3.3) and the Cauchy–Schwarz inequality, one has

$$\begin{aligned}\|\mathcal{H}U^n\|\le{}& \frac{(\lambda e^{-\varrho\tau}-\beta)e^{-\varrho(n-2)\tau}}{\lambda+\beta}\|\mathcal{H}U^0\|-\frac{(\lambda e^{-2\varrho\tau}-A_1)e^{-\varrho(n-3)\tau}}{\lambda+\beta}\|\mathcal{H}U^1\|\\&+\frac{A_2}{\lambda+\beta}\sum_{k=2}^{n-2}e^{-\varrho(n-k-2)\tau}\|\mathcal{H}U^k\|+\frac{A_3}{\lambda+\beta}\|\mathcal{H}U^{n-1}\|+\frac{1}{\lambda+\beta}\|\mathcal{H}f^n\|.\end{aligned} \tag{3.9}$$

Setting

$$B_k=\frac{A_2}{\lambda+\beta}e^{-\varrho(n-k-2)\tau} \quad \text{with } 2\le k\le n-2, \tag{3.10}$$

we have

$$\begin{aligned}\sum_{k=2}^{n-2} B_k\|\mathcal{H}U^k\| \\ &\leq B_2C_1\Big(\|\mathcal{H}U^0\| + \max_{1\leq s\leq 2}\|\mathcal{H}f^s\|\Big) + B_3C_2\Big(\|\mathcal{H}U^0\| + \max_{1\leq s\leq 3}\|\mathcal{H}f^s\|\Big) + \cdots \\ &\quad + B_{n-2}C_{n-3}\Big(\|\mathcal{H}U^0\| + \max_{1\leq s\leq n-2}\|\mathcal{H}f^s\|\Big).\end{aligned}$$

By Lemma 3.6, we have $0 < \sum_{k=2}^{n-2} B_k < 1$. Let $C = \max\{C_1, C_2, \dots, C_{n-3}\}$, which is independent of n. For the third term on the right-hand side of (3.9), we obtain

$$\begin{aligned}\sum_{k=2}^{n-2} B_k\|\mathcal{H}U^k\| &\leq (B_2 + B_3 + \cdots + B_{n-2})\, C\Big(\|\mathcal{H}U^0\| + \max_{1\leq s\leq n-2}\|\mathcal{H}f^s\|\Big) \\ &\leq \sum_{k=2}^{n-2} B_k\, C\Big(\|\mathcal{H}U^0\| + \max_{1\leq s\leq n-2}\|\mathcal{H}f^s\|\Big) \\ &\leq C\Big(\|\mathcal{H}U^0\| + \max_{1\leq s\leq n-2}\|\mathcal{H}f^s\|\Big).\end{aligned}$$

For the remaining terms on the right-hand side of (3.9), we just need to make sure that their coefficients are greater than zero and bounded. In fact, $\lambda e^{-\varrho\tau} - \beta > 0$ and Remark 3.7 imply that the coefficients of the remaining terms are greater than zero and bounded. In this way, we get

$$\|\mathcal{H}U^n\| \leq C\Big(\|\mathcal{H}U^0\| + \max_{1\leq s\leq n}\|\mathcal{H}f^s\|\Big) \quad \text{with } n \in [N]. \tag{3.11}$$

Similarly, if $k = n$ and $\lambda e^{-\varrho\tau} - \beta \leq 0$, using (3.4), by a similar proof, we also get the same result as (3.11).

Therefore, $\|\mathcal{H}U^n\| \leq C(\|\mathcal{H}U^0\| + \max_{1\leq s\leq n}\|\mathcal{H}f^s\|)$. Applying Lemma 3.3, we obtain

$$\|U^n\| \leq C\Big(\|U^0\| + \max_{1\leq s\leq n}\|f^s\|\Big).$$

The proof of this theorem is finished. □

We can derive the convergence of the discrete scheme (2.3) in a manner similar to the proof of Theorem 3.8.

Theorem 3.9. *Let u^n be the solution of equation (1.1) and let U^n be the solution of the CFD scheme for (2.3). Define $\varepsilon^n = u^n - U^n$, so that $\varepsilon^0 = 0$. Then*

$$\|\varepsilon^n\| \leq C(\tau^3 + h^4),$$

where C is a positive constant and $n \in [N]$.

Proof. Subtracting (2.3) from (2.2), we obtain

$$(\lambda+\beta)\mathcal{H}\varepsilon^n - a\delta_x^2\varepsilon^n = (\lambda e^{-\varrho\tau}-\beta)e^{-\varrho(n-2)\tau}\mathcal{H}\varepsilon^0 - (\lambda e^{-2\varrho\tau}-A_1)e^{-\varrho(n-3)\tau}\mathcal{H}\varepsilon^1 + A_2\sum_{k=2}^{n-2} e^{-\varrho(n-k-2)\tau}\mathcal{H}\varepsilon^k + A_3\mathcal{H}\varepsilon^{n-1} + R^n. \tag{3.12}$$

Multiplying both sides of (3.12) by $\mathcal{H}\varepsilon^n$ and integrating on Ω, we get

$$\begin{aligned}((\lambda+\beta)\mathcal{H}\varepsilon^n,\mathcal{H}\varepsilon^n) &- a(\delta_x^2\varepsilon^n,\mathcal{H}\varepsilon^n)\\ &= (\lambda e^{-\varrho\tau}-\beta)e^{-\varrho(n-2)\tau}(\mathcal{H}\varepsilon^0,\mathcal{H}\varepsilon^n) - (\lambda e^{-2\varrho\tau}-A_1)e^{-\varrho(n-3)\tau}(\mathcal{H}\varepsilon^1,\mathcal{H}\varepsilon^n)\\ &\quad + A_2\left(\sum_{k=2}^{n-2} e^{-\varrho(n-k-2)\tau}\mathcal{H}\varepsilon^k,\mathcal{H}\varepsilon^n\right) + A_3(\mathcal{H}\varepsilon^{n-1},\mathcal{H}\varepsilon^n) + (R^n,\mathcal{H}\varepsilon^n).\end{aligned} \tag{3.13}$$

In (3.13), since $-a(\delta_x^2\varepsilon^n,\mathcal{H}\varepsilon^n) = a(\varepsilon^n,\varepsilon^n)_A \geq 0$ and $\varepsilon^0 = 0$, by the Cauchy–Schwarz inequality and the result of Lemma 3.1, we obtain

$$\begin{aligned}(\lambda+\beta)\|\mathcal{H}\varepsilon^n\|^2 \leq &-(\lambda e^{-2\varrho\tau}-A_1)e^{-\varrho(n-3)\tau}\|\mathcal{H}\varepsilon^1\|\|\mathcal{H}\varepsilon^n\|\\ &+ A_2\sum_{k=2}^{n-2} e^{-\varrho(n-k-2)\tau}\|\mathcal{H}\varepsilon^k\|\|\mathcal{H}\varepsilon^n\| + A_3\|\mathcal{H}\varepsilon^{n-1}\|\|\mathcal{H}\varepsilon^n\|\\ &+ \|R^n\|\|\mathcal{H}\varepsilon^n\|,\end{aligned}$$

i.e.,

$$\begin{aligned}(\lambda+\beta)\|\mathcal{H}\varepsilon^n\| \leq &-(\lambda e^{-2\varrho\tau}-A_1)e^{-\varrho(n-3)\tau}\|\mathcal{H}\varepsilon^1\|\\ &+ A_2\sum_{k=2}^{n-2} e^{-\varrho(n-k-2)\tau}\|\mathcal{H}\varepsilon^k\| + A_3\|\mathcal{H}\varepsilon^{n-1}\| + \|R^n\|.\end{aligned} \tag{3.14}$$

Next, we use mathematical induction to prove $\|\mathcal{H}\varepsilon^n\| \leq C(\tau^3+h^4)$ with $n \in [N]$. For $n = 1$, by (3.14), we have

$$(2\lambda+\beta-A_1e^{2\varrho\tau})\|\mathcal{H}\varepsilon^1\| \leq A_3\|\mathcal{H}\varepsilon^0\| + \|R^1\| = \|R^1\|.$$

Since $\|R^n\| \leq C(\tau^3+h^4)$, we obtain

$$\|\mathcal{H}\varepsilon^1\| \leq \frac{1}{2\lambda+\beta-A_1e^{2\varrho\tau}}\|R^1\| \leq C(\tau^3+h^4).$$

Assume that

$$\|\mathcal{H}\varepsilon^k\| \leq C(\tau^3+h^4) \tag{3.15}$$

holds as $k = 2,\ldots,n-1$. We will show that $\|\mathcal{H}\varepsilon^n\| \leq C(\tau^3+h^4)$. By (3.10) and (3.15), the second term on the right-hand side of (3.14) can be obtained as

$$\sum_{k=2}^{n-2} B_k\|\mathcal{H}\varepsilon^k\| \leq B_2C_1(\tau^3+h^4) + B_3C_2(\tau^3+h^4) + \cdots + B_{n-2}C_{n-3}(\tau^3+h^4).$$

Let $C = \max\{C_1, C_2, \dots, C_{n-2}\}$ be a positive constant and independent of n; by (3.14)–(3.15) and Lemma 3.6, we obtain

$$\|\mathcal{H}\varepsilon^n\| \leq C(\tau^3 + h^4)\sum_{k=2}^{n-2} B_k + \|R^n\| \leq C(\tau^3 + h^4) + \|R^n\|.$$

Therefore, $\|\mathcal{H}\varepsilon^n\| \leq C(\tau^3 + h^4)$. Applying Lemma 3.3, we arrive at $\frac{1}{3}\|\varepsilon^n\|^2 \leq \|\mathcal{H}\varepsilon^n\|^2 \leq \|\varepsilon^n\|^2$, so that $\|\varepsilon^n\| \leq \sqrt{3}\|\mathcal{H}\varepsilon^n\|$, and then

$$\|\varepsilon^n\| \leq C(\tau^3 + h^4).$$

The proof of this theorem is thus finished. $\square$

The error estimation of our method with the Caputo–Fabrizio derivative and the same one in [27] with the Caputo derivative imply that we can get the following remark, which shows that the Caputo–Fabrizio derivative without singular term can improve the accuracy of the discrete scheme.

Remark 3.10. The temporal convergence rate (TCR) of our method is τ^3, and the TCR of the method in [27] is $\tau^{2-\alpha}$.

4. Numerical examples

In order to support our theoretical analysis in Section 3, we present some numerical examples in this section. Let $\tau = T/N$ be the time stepsize and $h = L/M$ the space stepsize, with N and M positive integers. For the numerical experiments, we used Matlab 2020a on a PC with an AMD Ryzen 5 3500U processor and 8 GB of memory. We use the following error norm:

$$E_n(\tau, h) = \max_{1\leq n\leq N} \|u^n - U^n\|.$$

Define the temporal convergence rate (TCR) by

$$\text{TCR} = \log(E_n(\tau_1, h)/E_n(\tau_2, h))/\log(\tau_1/\tau_2),$$

where $E_n(\tau_1, h)$ and $E_n(\tau_2, h)$ are the errors corresponding to mesh sizes τ_1 and τ_2, respectively. Similarly, define the spatial convergence rate (SCR) by

$$\text{SCR} = \log(E_n(\tau, h_1)/E_n(\tau, h_2))/\log(h_1/h_2),$$

where $E_n(\tau, h_1)$ and $E_n(\tau, h_2)$ are the errors corresponding to mesh sizes h_1 and h_2, respectively. Also, in order to investigate the SCR, we can use

$$\text{SCR} = \log(E_n(\tau_1, h_1)/E_n(\tau_2, h_2))/\log(h_1/h_2),$$

where $\tau_1 \ll h_1$ and $\tau_2 \ll h_2$ (we use $\tau = 1/1000$ in Table 2, and $\tau_1 = h_1^2$ and $\tau_2 = h_2^2$ in Table 4).

Example 4.1. In the first example, for $a = 1$ and $(x,t) \in [0,1]\times[0,1]$, the equation (1.1) will be

$$\begin{cases} {}_0^{\mathrm{CF}}D_t^{\alpha} u(x,t) = \dfrac{\partial^2 u}{\partial x^2} + f(x,t), \\ u(x,0) = 0, \\ u(0,t) = u(1,t) = 0, \end{cases}$$

where $f(x,t) = \sin(\pi x)\frac{3}{1-\alpha}(\frac{t^2}{\varrho} - \frac{2t}{\varrho^2} + \frac{2}{\varrho^3}(1-e^{-\varrho t})) + \pi^2 t^3 \sin(\pi x)$ and $\varrho = \frac{\alpha}{1-\alpha}$.

In this example, the exact solution of the equation can be obtained through calculation. However, in order to verify the effectiveness of our method, we assume that the exact solution of the equation is unknown and take the solution on the finer grid (that is, $M = N = 2000$) as the corresponding exact solution. First, the proposed scheme will be used to test the accuracy in the direction of time. In this case, we take $M = 200$. The errors, TCRs and CPU times at different α ($\alpha = 0.1$, 0.3, 0.5, and 0.7) are shown in Table 1. The data in Table 1 show that the TCR is about 3. Furthermore, we will test the accuracy of our scheme for space. We chose $N = 1000$ for $\alpha = 0.2$, 0.4, 0.6, and 0.8 at different M ($M = 10$, 20, 40, and 80). The errors, SCRs and CPU times are shown in Table 2. From Table 2 we can see that SCRs are $O(h^4)$. The above data indicates that the numerical experimental results are consistent with the theoretical analysis. A similar numerical example can be found in [27, Example 1], where the fractional derivative is the form of Caputo fractional derivative (with singular term). A comparison of the obtained results with other existing methods reveals that our method is more accurate and efficient for the time-fractional diffusion equation, where the fractional derivative is the form of Caputo–Fabrizio derivative (without singular term).

We present the solution on a finer grid (that is, $M = N = 2000$), the numerical solution ($M = 200$ and $N = 2000$), the absolute error and a contour plot of the absolute error in Figure 1, in which we use $\alpha = 0.02$. The error of numerical and exact solutions is small. In Figure 2 (a), we show the TCRs of Example 4.1 for $\alpha = 0.1, 0.3, 0.5$, and 0.7, respectively. In Figure 2 (b), we show the SCRs of Example 4.1 for $\alpha = 0.2, 0.4, 0.6$, and 0.8, respectively.

Example 4.2. For $a = 1$, $T = 1$ and $L = 1$, we want to consider the equation (1.1) with exact solution $u(x,t) = t^3 x^3 (1-x)^3$. Then the source term is

$$\begin{aligned} f(x,t) = {} & \frac{3}{1-\alpha} x^3 (1-x)^3 i\left(\frac{t^2}{\varrho} - \frac{2t}{\varrho^2} + \frac{2}{\varrho^3}(1-e^{-\varrho t})i\right) \\ & + 3t^3 x(1-x)\big(2(1-x)^2 - 6x(1-x) + 2x^2\big), \end{aligned}$$

where $\varrho = \frac{\alpha}{1-\alpha}$. The function $\varphi(x)$ can be found by the exact solution $u(x,t)$.

In order to verify TCRs, we fix the spatial meshes as $M = 1000$. We present the errors, TCRs and CPU times in Table 3. For different values of α, the TCRs of the CFD scheme reach the third order. In order to verify SCRs, we choose the spatial meshes M and temporal meshes N as $N = M^2$. The errors, SCRs and CPU times are shown in Table 4. For different values of α, the SCRs of the CFD scheme

TABLE 1. Errors, TCRs and CPU times for Example 4.1

	M	N	$E_n(\tau, h)$	TCR	CPU time
$\alpha = 0.1$	200	50	6.2229×10^{-8}	–	0.0603
		60	3.6062×10^{-8}	2.99	0.0807
		70	2.2686×10^{-8}	3.01	0.1039
		80	1.5145×10^{-8}	3.03	0.1240
$\alpha = 0.3$	200	50	2.6388×10^{-7}	–	0.0610
		60	1.5328×10^{-7}	2.98	0.0808
		70	9.6736×10^{-8}	2.99	0.0992
		80	6.4872×10^{-8}	2.99	0.1247
$\alpha = 0.5$	200	50	6.6895×10^{-7}	–	0.0627
		60	3.8869×10^{-7}	2.98	0.0777
		70	2.4543×10^{-7}	2.98	0.1026
		80	1.6471×10^{-7}	2.99	0.1259
$\alpha = 0.7$	200	50	1.6354×10^{-6}	–	0.0620
		60	9.4984×10^{-7}	2.98	0.0832
		70	5.9965×10^{-7}	2.98	0.1054
		80	4.0243×10^{-7}	2.99	0.1388

TABLE 2. Errors, SCRs and CPU times for Example 4.1

	M	N	$E_n(\tau, h)$	SCR	CPU time
$\alpha = 0.2$	10	1000	3.6409×10^{-5}	–	0.5056
	20		2.2689×10^{-6}	4.00	0.5842
	40		1.4172×10^{-7}	4.00	0.7930
	80		8.8756×10^{-9}	4.00	1.5948
$\alpha = 0.4$	10	1000	3.5612×10^{-5}	–	0.5024
	20		2.2192×10^{-6}	4.00	0.5903
	40		1.3858×10^{-7}	4.00	0.7865
	80		8.6458×10^{-9}	4.00	1.7361
$\alpha = 0.6$	10	1000	3.4486×10^{-5}	–	0.5081
	20		2.1489×10^{-6}	4.00	0.5872
	40		1.3412×10^{-7}	4.00	0.7849
	80		8.2944×10^{-9}	4.02	1.7771
$\alpha = 0.8$	10	1000	3.2843×10^{-5}	–	0.5218
	20		2.0464×10^{-6}	4.00	0.5998
	40		1.2751×10^{-7}	4.00	0.7798
	80		7.6744×10^{-9}	4.05	1.7200

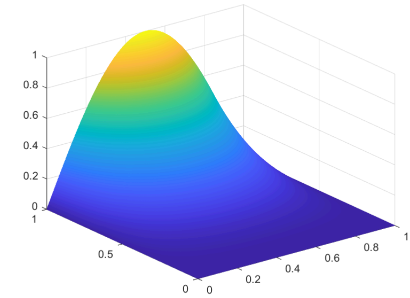

(a) Solution on finer grid

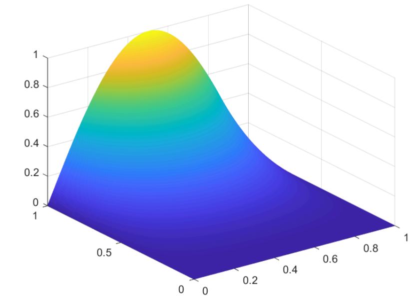

(b) Numerical solution

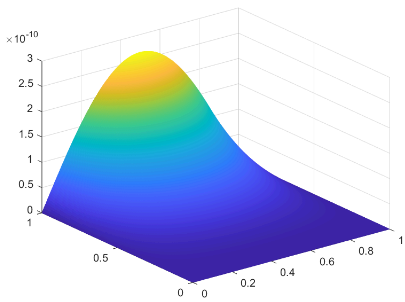

(c) Absolute error

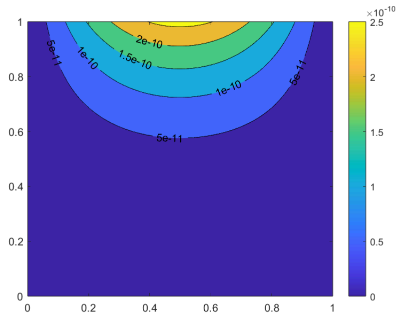

(d) Contour plot of absolute error

FIGURE 1. The results of Example 4.1 with $\alpha = 0.02$

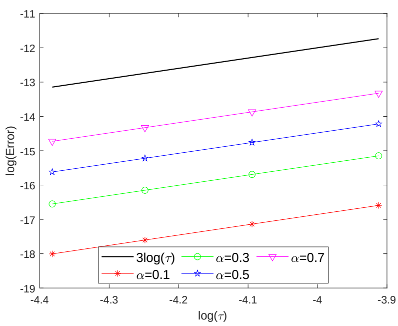

(a) $\alpha = 0.1, 0.3, 0.5, 0.7$

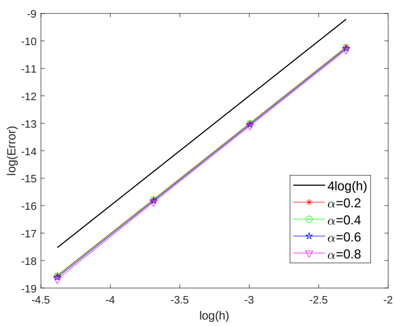

(b) $\alpha = 0.2, 0.4, 0.6, 0.8$

FIGURE 2. The TCRs and SCRs of Example 4.1 with given α

TABLE 3. Errors, TCRs and CPU times for Example 4.2

	M	N	L^∞-Error	L^∞-Rate	CPU time
$\alpha = 0.1$	1000	40	1.5563×10^{-9}	–	5.7114
		80	1.9781×10^{-10}	2.98	14.1234
		120	5.8767×10^{-11}	2.99	28.0687
		160	2.4749×10^{-11}	3.01	47.1467
$\alpha = 0.3$	1000	80	8.3603×10^{-10}	–	14.7304
		120	2.4876×10^{-10}	2.99	27.9238
		160	1.0492×10^{-10}	3.00	46.8027
		200	5.3733×10^{-11}	3.00	70.6237
$\alpha = 0.5$	1000	80	2.1186×10^{-9}	–	14.0054
		120	6.3084×10^{-10}	2.99	27.9049
		160	2.6649×10^{-10}	3.00	47.4357
		200	1.3652×10^{-10}	3.00	70.7949
$\alpha = 0.7$	1000	80	5.1671×10^{-9}	–	14.1410
		120	1.5381×10^{-9}	2.99	28.2142
		160	6.5040×10^{-10}	2.99	46.9748
		200	3.3332×10^{-10}	3.00	70.8377

reach the fourth order. The data of these tables show that our method provides an approximate solution with high accuracy for Example 4.2.

In Figure 3, we present the exact and numerical solutions, the absolute error and the contour plot of absolute error obtained from CFD scheme with $\alpha = 0.99$ at $M = 100$ and $N = 5000$. The results show that the numerical solution of the scheme has a high accuracy. In Figure 4 (a), we show the TCRs of Example 4.2 for $\alpha = 0.1, 0.3, 0.5$, and 0.7, respectively. In Figure 4 (b), we show the SCRs of Example 4.1 for $\alpha = 0.2, 0.4, 0.6$, and 0.8, respectively. Figure 4 indicates that the numerical solution produced by our method is in excellent agreement with the exact solution.

Example 4.3. In the third example, we consider the 2D case for (1.1), in which $T = 1$, $L = 1$, $u(\mathbf{x}, t) = t^4 \sin(\pi x)\sin(2\pi y)$, and $a = \sin(\pi t - \pi/2)$. Then the source term is

$$f(x, y, t) = \left(\frac{4}{1-\alpha}\left(\frac{t^3}{\sigma} - \frac{3t^2}{\sigma^2} + \frac{6t}{\sigma^3} - \frac{6}{\sigma^4}(1 - e^{-\sigma t})\right) + 5\pi^2 t^4 a\right)\sin(\pi x)\sin(2\pi y),$$

where $\sigma = \frac{\alpha}{1-\alpha}$. The function $\varphi(\mathbf{x})$ can be found by substituting $u(\mathbf{x}, t)$ into (1.1).

In order to verify TCRs in this example, we fix the spatial meshes as $M_1 = M_2 = M = 120$, where M_1 and M_2 denote the numbers of meshes in the x- and y-directions, respectively. We present the errors and TCRs in Table 5. From Table 5, we see that the TCRs of the CFD scheme reach the third order for different values of α. In order to verify SCRs, we choose the spatial meshes $M_1 = M_2 = M$ and

Table 4. Errors, SCRs and CPU times for Example 4.2

	M	N	L^∞-Error	L^∞-Rate	CPU time
$\alpha = 0.2$	10	100	3.3398×10^{-5}	–	0.0314
	20	400	2.0874×10^{-6}	4.00	0.2092
	40	1600	1.3046×10^{-7}	4.00	3.9552
	80	6400	8.1538×10^{-9}	4.00	133.7926
$\alpha = 0.4$	10	100	3.2643×10^{-5}	–	0.0266
	20	400	2.0402×10^{-6}	4.00	0.2169
	40	1600	1.2752×10^{-7}	4.00	3.9932
	80	6400	7.9697×10^{-9}	4.00	124.3089
$\alpha = 0.6$	10	100	3.1578×10^{-5}	–	0.0269
	20	400	1.9737×10^{-6}	4.00	0.2063
	40	1600	1.2336×10^{-7}	4.00	3.9823
	80	6400	7.7099×10^{-9}	4.00	124.0635
$\alpha = 0.8$	10	100	3.0023×10^{-5}	–	0.0259
	20	400	1.8767×10^{-6}	4.00	0.2090
	40	1600	1.1729×10^{-7}	4.00	3.9389
	80	6400	7.3310×10^{-9}	4.00	133.4166

Table 5. Errors and TCRs for Example 4.3

	M	N	L^∞-Error	L^∞-Rate
$\alpha = 0.3$	120	10	4.4542×10^{-6}	–
		15	1.3860×10^{-6}	2.88
		20	5.9047×10^{-7}	2.97
		25	2.9650×10^{-7}	3.09
$\alpha = 0.6$	120	10	2.1343×10^{-5}	–
		15	6.5900×10^{-6}	2.90
		20	2.8390×10^{-6}	2.93
		25	1.4659×10^{-6}	2.96
$\alpha = 0.9$	120	10	1.7720×10^{-4}	–
		15	5.2434×10^{-5}	3.00
		20	2.2203×10^{-5}	2.99
		25	1.1405×10^{-5}	2.99

temporal meshes $N = 300$. The errors and SCRs are shown in Table 6. From Table 6, we see that the SCRs of the CFD scheme reach the fourth order for different values of α. The data of these tables show that our method provides an approximate solution with high accuracy for the 2D case of (1.1).

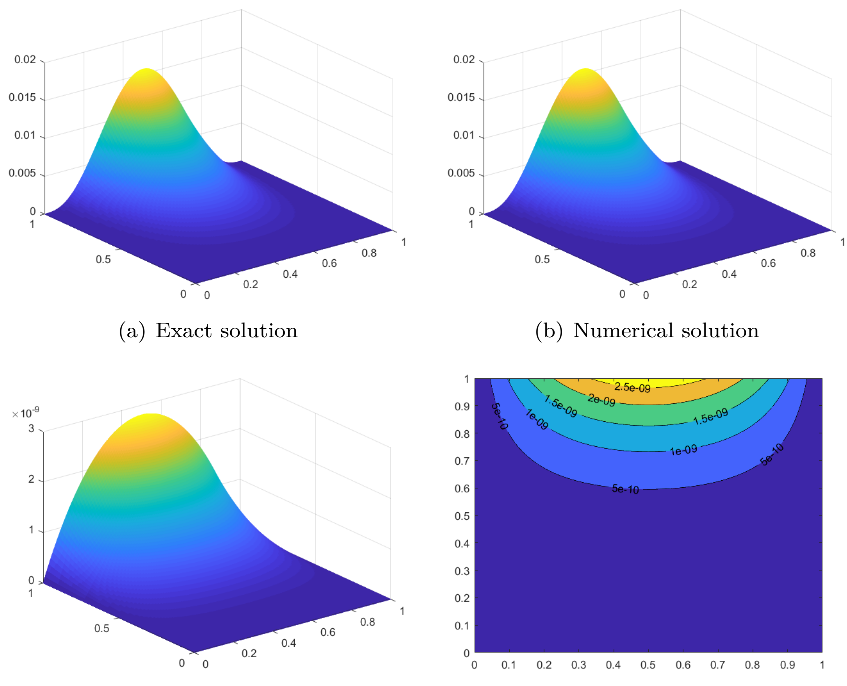

(a) Exact solution (b) Numerical solution

(c) Absolute error (d) Contour plot of absolute error

FIGURE 3. The results of Example 4.2 with $\alpha = 0.99$ at $M = 100$ and $N = 5000$

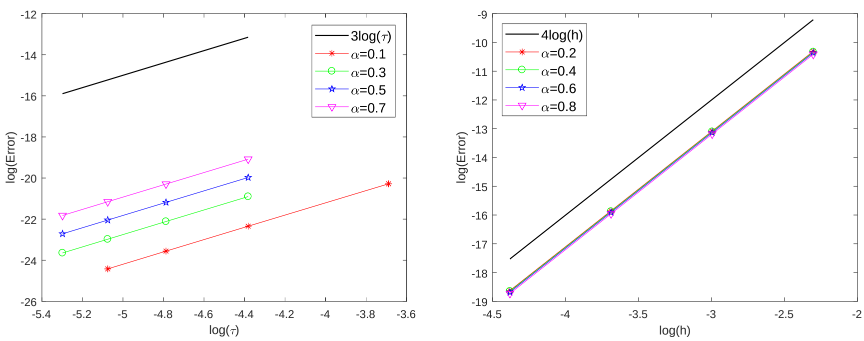

(a) $\alpha = 0.1, 0.3, 0.5, 0.7$ (b) $\alpha = 0.2, 0.4, 0.6, 0.8$

FIGURE 4. The TCRs and SCRs of Example 4.2 with given α

TABLE 6. Errors and SCRs for Example 4.3

	M	N	L^∞-Error	L^∞-Rate
$\alpha = 0.2$	10	300	5.2223×10^{-4}	–
	20		3.3923×10^{-5}	3.94
	30		6.6497×10^{-6}	4.01
	40		2.1139×10^{-6}	3.98
$\alpha = 0.5$	10	300	5.2736×10^{-4}	–
	20		3.4255×10^{-5}	3.95
	30		6.7145×10^{-6}	4.01
	40		2.1342×10^{-6}	3.98
$\alpha = 0.8$	10	300	5.3864×10^{-4}	–
	20		3.4986×10^{-5}	3.95
	30		6.8559×10^{-6}	4.01
	40		2.1776×10^{-6}	3.99

5. Conclusion

In this paper, we present a new CFD scheme for TFDEs. First, we develop a third-order approximation for the Caputo–Fabrizio derivative. For spatial discretization, we apply a fourth-order CFD scheme. The resulting method achieves third-order accuracy in time and fourth-order accuracy in space. We also prove that the scheme is stable. Finally, we provide numerical examples that confirm the correctness of the theoretical analysis. In future work, we will study numerical solutions of high-dimensional fractional differential equations and problems on complex domains.

References

[1] S. Abbas, M. Benchohra, and J. J. Nieto, Caputo–Fabrizio fractional differential equations with non instantaneous impulses, *Rend. Circ. Mat. Palermo (2)* **71** no. 1 (2022), 131–144. DOI MR Zbl

[2] T. Akman, B. Yildiz, and D. Baleanu, New discretization of Caputo–Fabrizio derivative, *Comput. Appl. Math.* **37** no. 3 (2018), 3307–3333. DOI MR Zbl

[3] A. Atangana, Non validity of index law in fractional calculus: A fractional differential operator with Markovian and non-Markovian properties, *Phys. A* **505** (2018), 688–706. DOI MR Zbl

[4] A. Atangana, Modelling the spread of COVID-19 with new fractal-fractional operators: Can the lockdown save mankind before vaccination?, *Chaos Solitons Fractals* **136** (2020), Paper No. 109860. DOI MR

[5] A. Atangana and J. Gómez-Aguilar, Decolonisation of fractional calculus rules: Breaking commutativity and associativity to capture more natural phenomena, *Eur. Phys. J. Plus* **133** (2018), Paper No. 166. DOI

[6] M. Caputo and M. Fabrizio, A new definition of fractional derivative without singular kernel, *Progr. Fract. Differentiation Appl.* **1** no. 2 (2015), 73–85.

[7] J. A. M. Carrer, B. S. Solheid, J. Trevelyan, and M. Seaid, A boundary element method formulation based on the Caputo derivative for the solution of the anomalous diffusion problem, *Eng. Anal. Bound. Elem.* **122** (2021), 132–144. DOI MR Zbl

[8] M. Cui, Compact finite difference method for the fractional diffusion equation, *J. Comput. Phys.* **228** no. 20 (2009), 7792–7804. DOI MR Zbl

[9] A. Daraghmeh, N. Qatanani, and A. Saadeh, Numerical solution of fractional differential equations, *Appl. Math. (Irvine)* **11** (2020), 1100–1115. DOI

[10] H. Dehestani and Y. Ordokhani, Pell–Lucas discretization method for finding the solution of Caputo–Fabrizio time-fractional diffusion equations, *Vietnam J. Math.* **52** no. 1 (2024), 235–254. DOI MR Zbl

[11] Z.-W. Fang, H.-W. Sun, and H. Wang, A fast method for variable-order Caputo fractional derivative with applications to time-fractional diffusion equations, *Comput. Math. Appl.* **80** no. 5 (2020), 1443–1458. DOI MR Zbl

[12] M. Fardi and J. Alidousti, A Legendre spectral-finite difference method for Caputo–Fabrizio time-fractional distributed-order diffusion equation, *Math. Sci. (Springer)* **16** no. 4 (2022), 417–430. DOI MR Zbl

[13] G.-H. Gao and H.-W. Sun, Three-point combined compact difference schemes for time-fractional advection-diffusion equations with smooth solutions, *J. Comput. Phys.* **298** (2015), 520–538. DOI MR Zbl

[14] R. Garrappa, Numerical solution of fractional differential equations: A survey and a software tutorial, *Mathematics* **6** no. 2 (2018), Paper No. 16. DOI Zbl

[15] R. Gorenflo, Y. Luchko, and M. Yamamoto, Time-fractional diffusion equation in the fractional Sobolev spaces, *Fract. Calc. Appl. Anal.* **18** no. 3 (2015), 799–820. DOI MR Zbl

[16] R. Gorenflo, F. Mainardi, D. Moretti, and P. Paradisi, Time fractional diffusion: A discrete random walk approach, *Nonlinear Dynam.* **29** no. 1-4 (2002), 129–143. DOI MR Zbl

[17] B. Guo, X. Pu, and F. Huang, *Fractional partial differential equations and their numerical solutions*, World Scientific, Hackensack, NJ, 2015. DOI MR Zbl

[18] S. Guo, L. Mei, Y. Li, and Y. Sun, The improved fractional sub-equation method and its applications to the space-time fractional differential equations in fluid mechanics, *Phys. Lett. A* **376** no. 4 (2012), 407–411. DOI MR Zbl

[19] M. S. Hashemi, A novel approach to find exact solutions of fractional evolution equations with non-singular kernel derivative, *Chaos Solitons Fractals* **152** (2021), Paper No. 111367. DOI MR Zbl

[20] R. Hilfer (ed.), *Applications of fractional calculus in physics*, World Scientific, Singapore, 2000. DOI MR Zbl

[21] J. Hristov, Derivatives with non-singular kernels from the Caputo–Fabrizio definition and beyond: Appraising analysis with emphasis on diffusion models, in *Frontiers in fractional calculus*, Curr. Dev. Math. Sci. 1, Bentham Sci. Publ., Sharjah, 2018, pp. 269–341. DOI MR Zbl

[22] D. Hu and X. Cao, A fourth-order compact ADI scheme for two-dimensional Riesz space fractional nonlinear reaction-diffusion equation, *Int. J. Comput. Math.* **97** no. 9 (2020), 1928–1948. DOI MR Zbl

[23] A. Jannelli, M. Ruggieri, and M. P. Speciale, Numerical solutions of space-fractional advection-diffusion equations with nonlinear source term, *Appl. Numer. Math.* **155** (2020), 93–102. DOI MR Zbl

[24] A. A. Kosov and È. I. Semenov, Exact solutions of the nonlinear diffusion equation, *Sib. Math. J.* **60** no. 1 (2019), 93–107, translation from *Sib. Mat. Zh.* **60** no. 1 (2019), 123–140. DOI MR Zbl

[25] S. Kumar, A. Kumar, B. Samet, J. F. Gómez-Aguilar, and M. S. Osman, A chaos study of tumor and effector cells in fractional tumor-immune model for cancer treatment, *Chaos Solitons Fractals* **141** (2020), Paper No. 110321. DOI MR Zbl

[26] Y. Li, F. Liu, I. W. Turner, and T. Li, Time-fractional diffusion equation for signal smoothing, *Appl. Math. Comput.* **326** (2018), 108–116. DOI MR Zbl

[27] Y. Lin and C. Xu, Finite difference/spectral approximations for the time-fractional diffusion equation, *J. Comput. Phys.* **225** no. 2 (2007), 1533–1552. DOI MR Zbl

[28] J. Liu, J. Zhang, and X. Zhang, Semi-discretized numerical solution for time fractional convection-diffusion equation by RBF-FD, *Appl. Math. Lett.* **128** (2022), Paper No. 107880. DOI MR Zbl

[29] Y. Luchko, Initial-boundary-value problems for the one-dimensional time-fractional diffusion equation, *Fract. Calc. Appl. Anal.* **15** no. 1 (2012), 141–160. DOI MR Zbl

[30] V. Mehandiratta and M. Mehra, A difference scheme for the time-fractional diffusion equation on a metric star graph, *Appl. Numer. Math.* **158** (2020), 152–163. DOI MR Zbl

[31] H. Mohammadi, S. Kumar, S. Rezapour, and S. Etemad, A theoretical study of the Caputo–Fabrizio fractional modeling for hearing loss due to mumps virus with optimal control, *Chaos Solitons Fractals* **144** (2021), Paper No. 110668. DOI MR

[32] K. M. Owolabi and A. Atangana, Numerical approximation of nonlinear fractional parabolic differential equations with Caputo–Fabrizio derivative in Riemann–Liouville sense, *Chaos Solitons Fractals* **99** (2017), 171–179. DOI MR Zbl

[33] I. Podlubny, *Fractional differential equations*, Math. Sci. Eng. 198, Academic Press, San Diego, CA, 1999. MR Zbl

[34] M. Ran and C. Zhang, New compact difference scheme for solving the fourth-order time fractional sub-diffusion equation of the distributed order, *Appl. Numer. Math.* **129** (2018), 58–70. DOI MR Zbl

[35] M. Shafiq, F. A. Abdullah, M. Abbas, A. Sm Alzaidi, and M. B. Riaz, Memory effect analysis using piecewise cubic B-spline of time fractional diffusion equation, *Fractals* **30** no. 8 (2022), Paper No. 2240270. DOI Zbl

[36] J. Shi and M. Chen, A second-order accurate scheme for two-dimensional space fractional diffusion equations with time Caputo–Fabrizio fractional derivative, *Appl. Numer. Math.* **151** (2020), 246–262. DOI MR Zbl

[37] Z. Soori and A. Aminataei, Two new approximations to Caputo–Fabrizio fractional equation on non-uniform meshes and its applications, *Iran. J. Numer. Anal. Optim.* **11** no. 2 (2021), 365–383. DOI Zbl

[38] H. Sun, A. Chang, Y. Zhang, and W. Chen, A review on variable-order fractional differential equations: Mathematical foundations, physical models, numerical methods and applications, *Fract. Calc. Appl. Anal.* **22** no. 1 (2019), 27–59. DOI MR Zbl

[39] M. Taghipour and H. Aminikhah, A new compact alternating direction implicit method for solving two dimensional time fractional diffusion equation with Caputo–Fabrizio derivative, *Filomat* **34** no. 11 (2020), 3609–3626. DOI MR Zbl

[40] Z. Wang and S. Vong, Compact difference schemes for the modified anomalous fractional sub-diffusion equation and the fractional diffusion-wave equation, *J. Comput. Phys.* **277** (2014), 1–15. DOI MR Zbl

[41] Y. Yan, K. Pal, and N. J. Ford, Higher order numerical methods for solving fractional differential equations, *BIT* **54** no. 2 (2014), 555–584. DOI MR Zbl

[42] H. Ye, F. Liu, and V. Anh, Compact difference scheme for distributed-order time-fractional diffusion-wave equation on bounded domains, *J. Comput. Phys.* **298** (2015), 652–660. DOI MR Zbl

[43] P. Zhang and H. Pu, A second-order compact difference scheme for the fourth-order fractional sub-diffusion equation, *Numer. Algorithms* **76** no. 2 (2017), 573–598. DOI MR Zbl

[44] X. Zhao, Z.-Z. Sun, and Z.-P. Hao, A fourth-order compact ADI scheme for two-dimensional nonlinear space fractional Schrödinger equation, *SIAM J. Sci. Comput.* **36** no. 6 (2014), A2865–A2886. DOI MR Zbl

Xindong Zhang✉
College of Big Data Statistics, Guizhou University of Finance and Economics, Guiyang, 550025, People's Republic of China
liaoyuan1126@163.com

Hanxiao Wang
School of Mathematical Sciences, Xinjiang Normal University, Urumqi, 830017,
People's Republic of China
984212575@qq.com

Ziyang Luo
School of Mathematics and Physics, Xinjiang Institute of Engineering, Urumqi, 830023,
People's Republic of China
466949841@qq.com

Leilei Wei
College of Science, Henan University of Technology, Zhengzhou, 450001,
People's Republic of China
leileiwei@haut.edu.cn

Received: February 17, 2024
Accepted: June 18, 2024
Early view: September 3, 2024